Guest Forum

Context Microscopy and Fingerprinting Spectroscopy of Micro- and Nanoplastics and Their Effects on Human Kidney Cells Using nanoGPS and ParticleFinder

マイクロプラスチックの光学顕微鏡による形態観察と分光法による化学同定ならびに
nanoGPSとParticleFinderを用いたマイクロプラスチックのヒト腎臓細胞への影響評価

George SARAU, Ph.D.[§]
ゲオルグ ザロ

Fraunhofer Institute for Ceramic Technologies and Systems IKTS, Max Planck Institute for the Science of Light, Institute for Nanotechnology and Correlative Microscopy eV INAM

Melina YARBAKHT, Ph.D.[§]
メリーナ ヤバークト

Department of Nephrology, University Hospital, Friedrich-Alexander University Erlangen-Nürnberg (FAU), Translation Research Center

Barbara E. OßMANN, Ph.D.
バーバラ E オスマン

Max Planck Institute for the Science of Light, Bavarian Health and Food Safety Authority
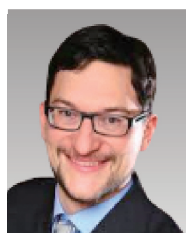
Lasse KLING
ラッセ クリング

Max Planck Institute for the Science of Light, Institute for Nanotechnology and Correlative Microscopy eV INAM

Johannes AST, Ph.D.
ヨハネス アスト

Fraunhofer Institute for Ceramic Technologies and Systems IKTS, Institute for Nanotechnology and Correlative Microscopy eV INAM

Florian VOLLNHALS, Ph.D.
フロリアン フォルンハルツ

Institute for Nanotechnology and Correlative Microscopy eV INAM Institute of Optics, Information and Photonics, Friedrich-Alexander University Erlangen-Nürnberg (FAU)

Janina MUELLER-DEILE, MD
ジャニナ ムエラ ダイレ

Department of Nephrology, University Hospital, Friedrich-Alexander University Erlangen-Nürnberg (FAU), Translation Research Center

Mario SCHIFFER, MD,MBA
マリオ シファー

Department of Nephrology, University Hospital, Friedrich-Alexander University Erlangen-Nürnberg (FAU), Translation Research Center

Silke H. CHRISTIANSEN, Ph.D.
ジルク H クリスティアンセン

Fraunhofer Institute for Ceramic Technologies and Systems IKTS, Max Planck Institute for the Science of Light, Institute for Nanotechnology and Correlative Microscopy eV INAM Physics Department, Freie Universität Berlin

§ These authors contributed equally to this work.

Nowadays humans are almost continuously exposed to micro- and nanoplastics (MNPs) through food and air, but very little is known about the exposure level and impact on our health. Here, we focus on bottled mineral water and cultured human podocytes as representative kidney cells prone to accumulation of particles. It is demonstrated that identical MNPs and cells can be precisely relocalized and extensively characterized down to nanoscale in independent instruments using nanoGPS and ParticleFinder technologies developed by HORIBA. Reference particles and particles contained in mineral water were detected, enabling statistical distributions of their mean number, size, and type depending on the bottle and

Guest Forum
特別寄稿

Context Microscopy and Fingerprinting Spectroscopy of Micro- and Nanoplastics and Their Effects on Human Kidney Cells Using nanoGPS and ParticleFinder

label materials. The primary effects of MNPs (three standards and tyre wear) on human podocytes were assessed using a cell viability test followed by correlative microscopy and spectroscopy investigations of the same cells. We observed changes in the biological features of MNP treated cells compared to non-treated controls, attributed to cell damage through surface adhesion and uptake of plastic particles. The integration of automatic relocalization and detection of identical objects in a multi-instrument workflow represents a novel analytical approach that can be applied beyond this topic.

Key words
microplastic, nanoplastic, tyre wear, podocytes, kidney, nanoGPS, ParticleFinder, SEM, Raman, correlative workflow, microscopy, spectroscopy

現在，我々は食品や大気を通して，マイクロ～ナノサイズという非常に小さい粒子（MNPs）に日常的に曝されている。しかしながらどの程度曝されているのか，またそれが我々の健康にどの様な影響を及ぼしているかは，ほとんど知られていない。我々は，HORIBAが開発したnanoGPSとParticle Finderの2つの技術を使い，測定対象に対し，正確に位置合わせを行うことで，独立した機器で同一のMNPsをナノスケールまでかつ広範囲にわたり解析を実現した。本項では，容器入り天然水と，粒子の蓄積が起こりやすい代表的な腎臓細胞として培養ヒト有足細胞の2つについて解析を行った結果を示す。まず，リファレンス粒子及び天然水ボトルにふくまれるMNPsを検出し，ボトルやラベルの材質に依存した平均粒子数やサイズ，種類に関する統計解析を行い，その性能を実証した。次いで，ヒト由来ポドサイトに対するMNPs（3種の標準粒子と摩耗タイヤから得た粒子使用）の主な影響は細胞生存率試験で評価され，その同じ細胞を相関顕微鏡法と分光法で解析した（顕微画像とスペクトル測定の同期技術により，対象細胞に関する複数の情報を同一視野角で取得している）。MNPsと共に調製された細胞と無調製の細胞を比較し，MNPsの付着や取り込みによる細胞へのダメージに帰属できる状態の変化を観察し，MNPsの生物学的特徴を評価した。複数の機器を用いた測定により，同一の測定対象の位置合わせだけでなく，自動化できる本技術は，本事例にとどまらず，広く活用が期待される新規分析手法である。

キーワード
マイクロプラスチック，ナノプラスチック，タイヤ摩耗，ポッドサイト，腎臓，nanoGPS，パーティクルファインダー，SEM，ラマン，相関ワークフロー，顕微鏡，分光法

Introduction

Production of plastics has dramatically increased over the last decades and with it the plastic waste in the environment.[1] Plastics are nowadays used almost in all products including packaging, construction, textiles, tires, cosmetics, and so on.[2-4] The major issue is the mismanaged plastic waste that is not collected at all or improperly filtered and recycled, which significantly contaminates the environment on a global scale through the transfer between terrestrial, river, and ocean compartments.[5] Once left in the environment, plastic debris persists and degrades continuously into smaller fragments down to micro- and nanoplastic (MNP) particles, attributed to size classes of < 5 mm and < 1 μm or ≤ 100 nm, respectively.[6,7] With time, these MNPs are assumed to develop into toxic chemical cocktails by increased adsorption of hazardous pollutants and pathogens from the environment given their larger surface areas due to fragmentation, in addition to additives and pigments added during manufacturing of plastics. Moreover, the smaller the plastic particles become (< 1.5 μm), the higher the probability to enter by ingestion and inhalation into human organs and subse-

quently to accumulate and leach chemicals with still unknown toxicological effects on our health.[8-10]

Microscopy- and spectroscopy-based methods are commonly used to monitor MNPs in environmental samples usually after filtering as well as in various biological matrices and organisms. The employed techniques mainly include optical microscopy with stereozoom, scanning electron microscopy (SEM) with energy dispersive X-ray spectroscopy (EDS), pyrolysis gas chromatography coupled with mass spectrometry (py-GC-MS), Fourier-transform infrared (FT-IR) and Raman microspectroscopies, each method with its benefits and drawbacks.[11-13] Recently, we showed that a correlative approach is needed to avoid overestimation of particles' size and underestimation of particles' number for clustered MNPs as well as to measure Raman without optically visualizing the plastic nanoparticles by overlapping SEM and optical images of high (< 10 nm) and low (~ 1 μm) spatial resolution, respectively. This was achieved by a correlative microscopy and spectroscopy workflow applied to identical MNP particles on large-area filters using an optical zoom microscope and a hyphenated

SEM-Raman instrument (with a bright field optical objective for micro-Raman inside the SEM vacuum chamber).[14] However, such combined systems are limited with respect to the number of measurement techniques available on one instrument compared to stand-alone, method-specific instruments from different manufacturers, in which finding the same micro- and nanosized objects is still a challenge.[15-19]

In this work, the first application of a newly developed relocalization technology for a detailed characterization of MNPs and their effects on human kidney cells in independent instruments is demonstrated. This technology is based on a patented position encoder tag (from HORIBA), called nanoGPS tag, with lithographically defined patterns. These patterns are used to translate the sample coordinates corresponding to the regions of interest (ROIs) into the stage coordinates of different instruments (from HORIBA, Zeiss, Leica in this study), regardless of the sample orientation. Furthermore, the applicability of the ParticleFinder software module (from HORIBA) for automatic detection of microplastic (MP), pigment, and additive particles on large-area filters is shown. Context microscopy and fingerprinting spectroscopy approaches were applied to standard MPs, microparticle contamination of bottled mineral water, and human podocytes that were either untreated or incubated with MNPs. The podocytes exposed to MNPs were under stress and started to die gradually, indicating an overall effect of particle exposure on cell viability.

Experimental

The samples investigated in this study can be divided into three categories: reference micro-sized plastic particles, mineral water from different bottle types bought in Bavarian food stores, and human podocytes cell cultures exposed to MNPs.

Standard MP particles
Commercially available standard plastics (see Table 1) were selected to match the polymer types routinely encountered in the environment.[13,20,21] A mixture of polyethylene (PE), poly(vinyl chloride) (PVC), polyamide-Nylon 6 (PA), polystyrene (PS), and polypropylene (PP) particles were suspended in a solution (ultrapure water and sodium dodecyl sulphate (SDS)) followed by vacuum filtration through polycarbonate (PC) membrane filters (diameter 25 mm, pore size 0.4 μm) previously coated with aluminum (Al thickness 100 nm) as detailed in our previous work.[22] These reference materials were used to evaluate the nanoGPS relocalization technology (hardware and software) and its integration in a correlative microscopy and spectroscopy workflow applied to identical MNP particles (see Figure 1). The nanoGPS tag (4×5 mm^2 silicon piece) is firmly attached next to the filter, which is rigidly stretched and flattened between two metal rings fixed on a SEM holder, to avoid any thermal drift and ensure precise relocalization in different instruments. Along with the corresponding NaviGo software, the instruments' stages involved in the workflow are calibrated and the coordinates of ROIs are recorded.

Mineral water particles
Real mineral water samples packaged in reusable bottles made of poly(ethylene terephthalate) (PET), in single use PET bottles, and in glass bottles (single and reusable) were analyzed for microparticle contamination, taking also into account bottle age as well as label and cap type. Before suspension in SDS solution and vacuum filtration through Al coated PC membranes, calcium and magnesium carbonate particles were dissolved with ethylene diamine tetraacetic acid tetrasodium salt (EDTA) to reduce the number of non-plastic particles.[21] To obtain statistically relevant data given the complexity of bottled mineral water contamination including microplastic, pigment, additive, and mixed particles, we employed an automatic particle detection approach. This is based on the ParticleFinder software that transforms large-area (1 mm^2) dark field optical images obtained by stitching into grey scale images, on which particles are easily detectable using their brightness, counted, classified by size and shape, and their coordinates recorded for further micro-Raman chemical identification. Thus, the mean

Table 1   Details of the plastic particle standards used in the present study to assess the nanoGPS relocalization and the exposure of human podocytes to plastics (PVC, PA, PP). Adapted with permission from Springer Nature.[22]

Material	Type	Manufacturer	Size (μm)
Polyethylene (PE)	Clear microspheres, powder	Cospheric	1-10
			10-106
Poly (vinyl chloride) (PVC)	Powder	Pyropowders.de	< 50
Polyamide - Nylon 6 (PA)	Powder	GoodFellow	15-20 (average particle size)
Polystyrene (PS)	Polybead Micron Microspheres, 2.5% solids in water	Polysciences Inc.	1
Polypropylene (PP)	Chromatographic Grade, powder	Polysciences Inc.	25-85

Guest Forum
特別寄稿

Context Microscopy and Fingerprinting Spectroscopy of Micro- and Nanoplastics and Their Effects on Human Kidney Cells Using nanoGPS and ParticleFinder
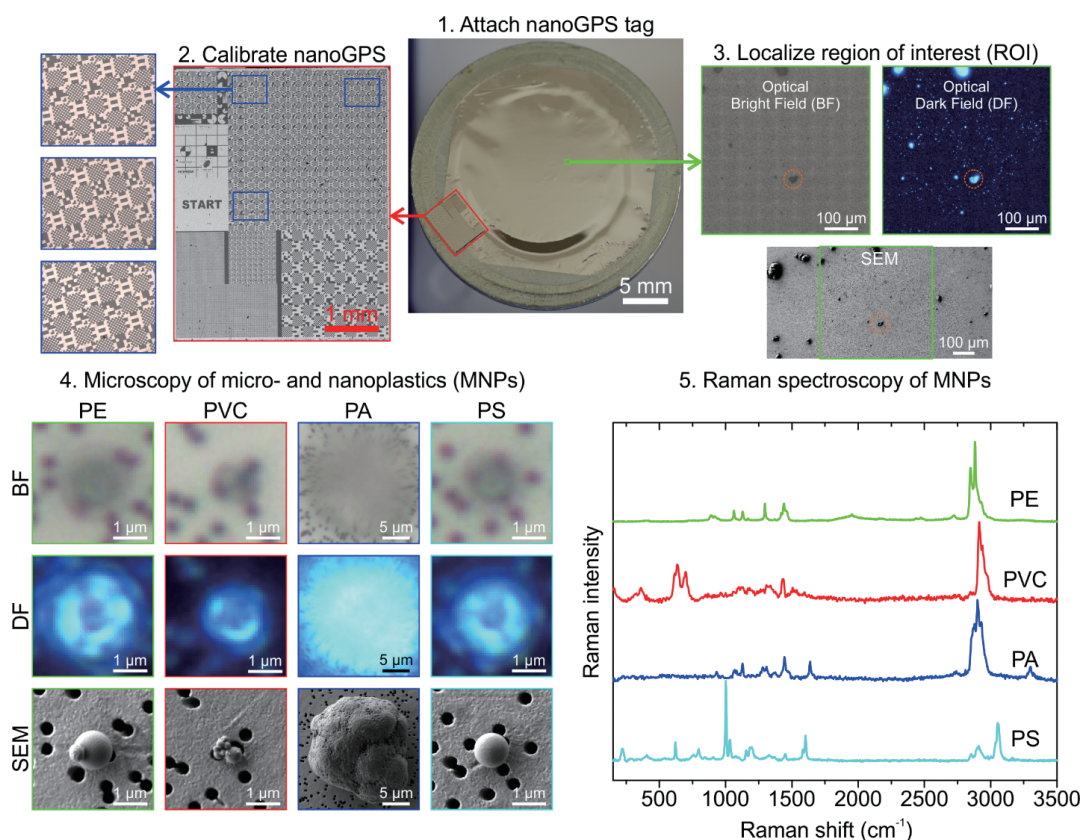

Figure 1 Correlative microscopy and spectroscopy workflow for micro- and nanoplastics on an Al coated PC membrane used to filter MNPs from water. First, a so-called nanoGPS tag is attached directly to the sample. Second, three images are recorded at random positions on a pattern (different patterns correspond to various instrument magnifications) and fed into a software that calibrates the global, stage coordinates into local, tag (sample) coordinates including sample rotation. This procedure is repeated for each instrument to be used in the workflow. Third, identical ROIs are precisely relocalized in independent instruments, regardless of the sample orientation. Fourth, the same single or agglomerated particles are imaged at optical (BF, DF) and SEM spatial resolutions to assess size, shape, number, and surface morphology of MNPs down to nanoscale. DF imaging is used to clearly distinguish MNPs from the porous structure of large-area filters. Fifth, unambiguously chemical identification by micro-Raman spectroscopy is applied. The Raman spectra are taken with permission from the Society for Applied Spectroscopy.[14]

number of microplastic, pigmented, and additive particles (projected to 1 L sample volume), their size, and type distributions were estimated (see **Figure 2**, additives not included).[21,22]

Human podocytes exposure to MNPs

Conditionally immortalized human podocytes that contain a heat sensitive CV40T antigen were cultured as described previously.[23] Podocytes were proliferated under growth permissive conditions at 33°C and further differentiated through the inactivation of SV40 T-antigen at 37°C. After 7 days of differentiation, cells were treated with different concentrations of diluted standard plastic (PVC: 0.5, 1 mg/ml; PA: 0.5, 1 mg/ml; PP: 2.5, 5 mg/ml) and tyre wear (0.125, 0.5 mg/ml) particles for 7 h to evaluate their possible effects on the cells. In order to decrease the aggregation of particles, they were sonicated before the incubation. Following the particle treatment, cells were washed two to three times with phosphate buffered saline (PBS) and fixed for further biological, imaging, and spectroscopy assays. For this study, the podocytes were grown on the surface of silicon wafers previously coated with platinum (Pt thickness 100 nm) that were attached along with nanoGPS tags to SEM holders to avoid relative sample - tag position shifts when moving between instruments.

Analytical methods

Complementary analytical techniques present on different instruments were used to visualize and detect MNPs on filters and inside cells as well as to determine the changes in cells caused by the contact with MNPs. All measurements have been performed at room temperature. The latter point was first addressed by using a live-dead cell imaging kit based on two-color fluorescence cell viability assay (Thermo Fischer Scientific). Based on this assay, cell-permeable and cell-impermeable dyes were used for staining of live and dead/dying cells, respectively. Following the particle treatment, the live/dead cells were assigned based on the kit instruction. Fluorescent images were collected with the use of an Evos M5000 imaging microscope (Thermo Fischer Scientific) (see **Figure 3**).

Furthermore, we employed a confocal micro-Raman spectrometer (HORIBA LabRAM HR Evo-Nano or XploRa PLUS), operated by the LabSpec 6 software (with

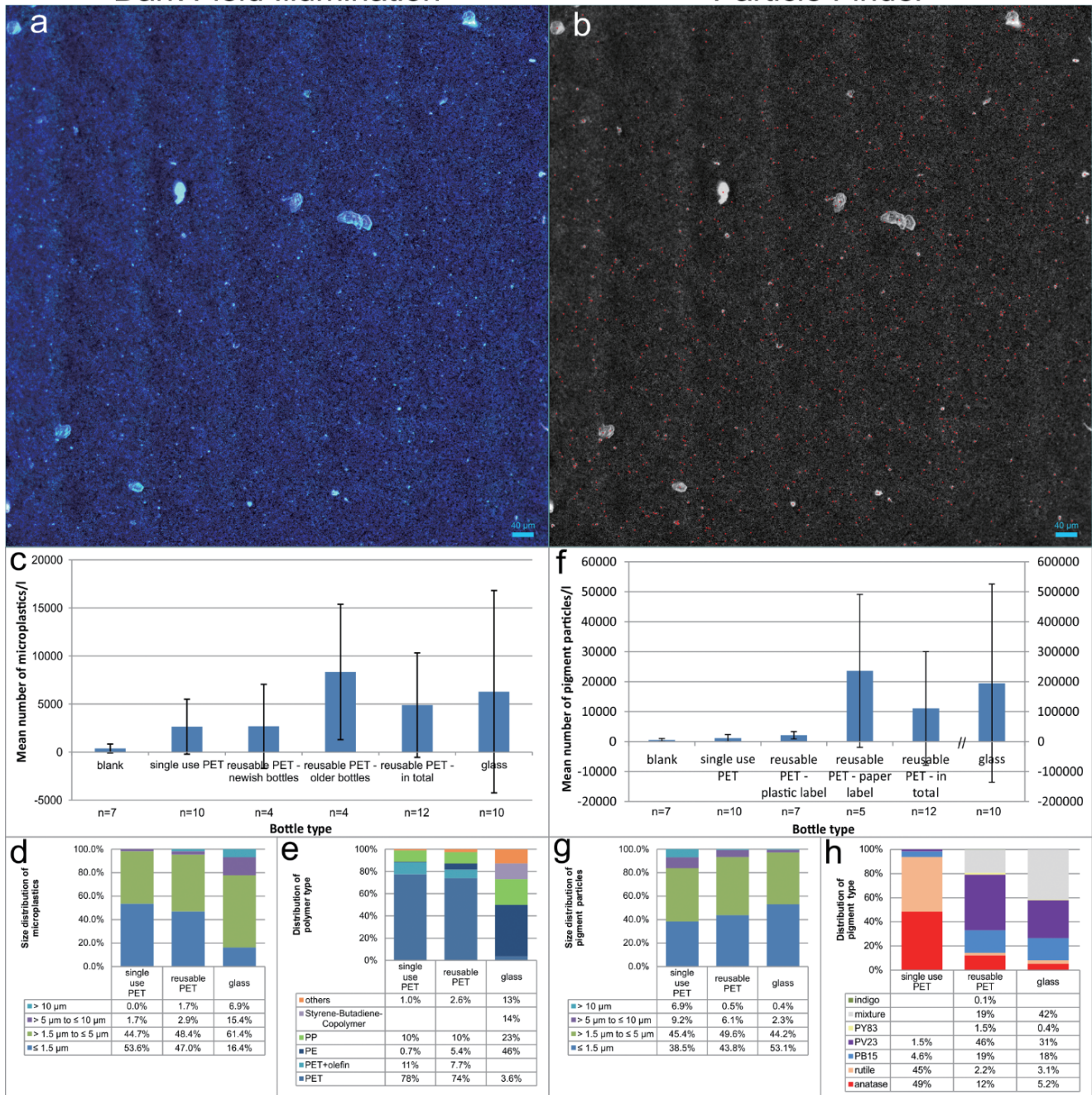## Dark Field Illumination

Particle Finder

Figure 2 (a) Example of a dark field montage (1 mm²) obtained by stitching, on which particles from mineral water samples shine brighter than the pores of the Al coated PC membrane filter. (b) ParticleFinder software converts the DF image into a grey scale image used to automatically detect, classify, and measure Raman spectra of individual particles at their center, marked by red points. (c, d, e) Mean number of microplastics ± standard deviation projected to 1 L sample volume, size, and plastic type distributions function of the bottle material. (f, g, h) Mean number of pigments ± standard deviation projected to 1 L sample volume, size, and pigment type distributions function of the bottle material. Adapted with permission from Elsevier.[21]

data analysis and ParticleFinder), equipped with bright and dark field illumination (BF, DF) objectives coupled to a camera to image MNPs and cells (~ 1 μm spatial resolution). Three lasers (532, 633, and 785 nm) focused by 50× (NA 0.75) or 100× (NA 0.9) objectives were used for Raman excitation and collection in a backscattering geometry with laser powers of 1.2 mW or 3.2 mW (532 nm), 11.2 mW (633 nm), and 5.3 mW (785 nm). Two gratings (300 and 600 grooves/mm) and integration times of 1 - 20 s and 2x accumulations were applied. The acquired Raman spectra and maps (step size 1 μm) were analyzed

to chemically identify the particles and the structural damage induced by them on the human podocytes. A SEM (Zeiss field emission Auriga, secondary electron detector) was used for a detailed morphological imaging of MNPs and cells (< 10 nm spatial resolution) at a low voltage of 1 kV to avoid modifications caused by electron scanning. The height profiles of the same cells investigated by micro-Raman and SEM were measured by a confocal imaging microscope (Leica DCM 3D), the relocalization of identical cells being realized using the nanoGPS technology (see Figure 4). Moreover, because

uest Forum
特別寄稿
G

Context Microscopy and Fingerprinting Spectroscopy of Micro- and Nanoplastics and Their Effects on Human Kidney Cells Using nanoGPS and ParticleFinder

of the superposition of Raman bands related to the plastic materials and cells, we applied a classical least squares algorithm (CLS) available in LabSpec 6 to highlight the

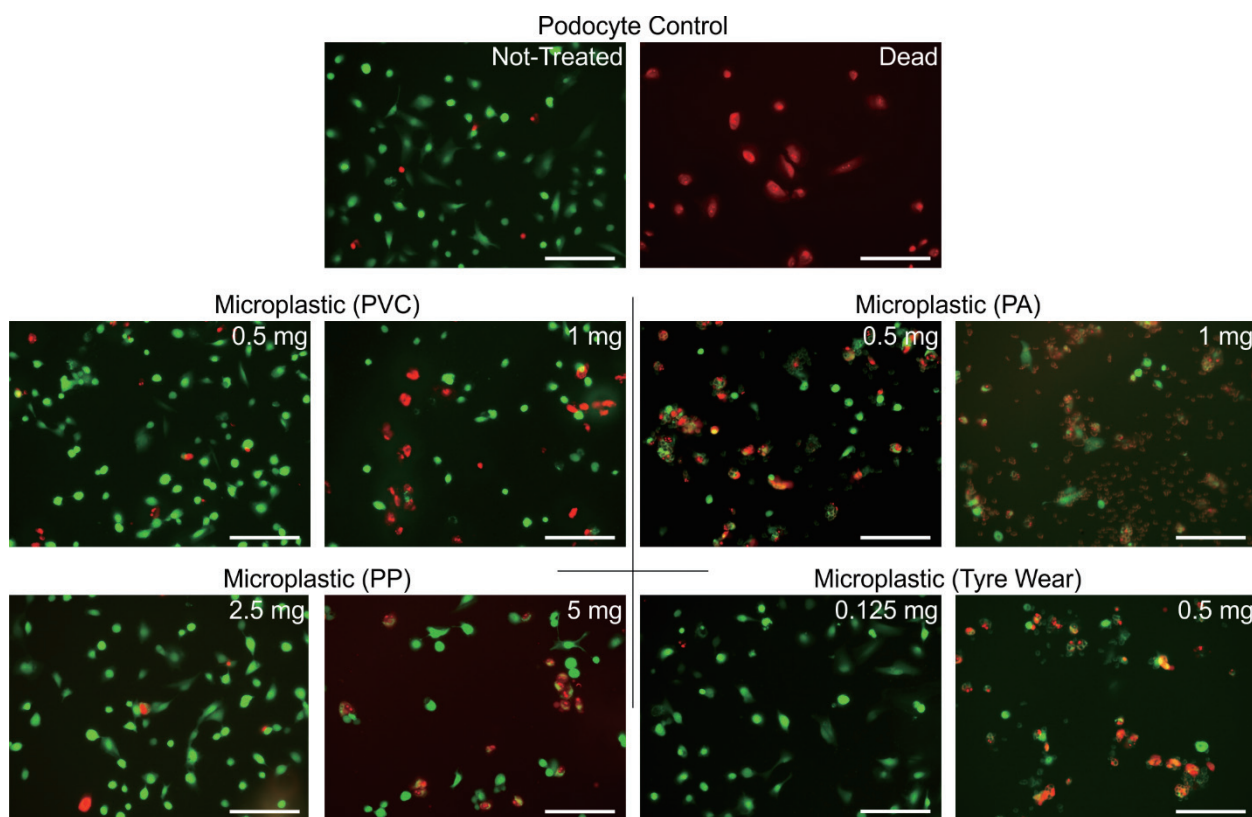spatial distribution of MNPs on the mapped cells (see Figure 5).

Figure 3   Fluorescence live - dead cell imaging (green - red) to assay the cytotoxicity of microplastic and tyre wear particles on podocytes, following 7 h particle exposure at relevant concentrations (mg/ml) and washing with PBS. The control cells were non-treated or intentionally killed to check the live - dead cell imaging kit. The concentrations to initiate and induce a notable impact on podocytes depends on the polymer type. During particle incubation the cells are under stress and start to die gradually. Consequently, some of the degraded cells are washed away and not assigned with colors. Some attached particles with intrinsic fluorescence are also visible. The preliminary results of this assay are yet mostly qualitative and show an overall effect of particle treatment on the cell viability. Scale bars are 300 μm.
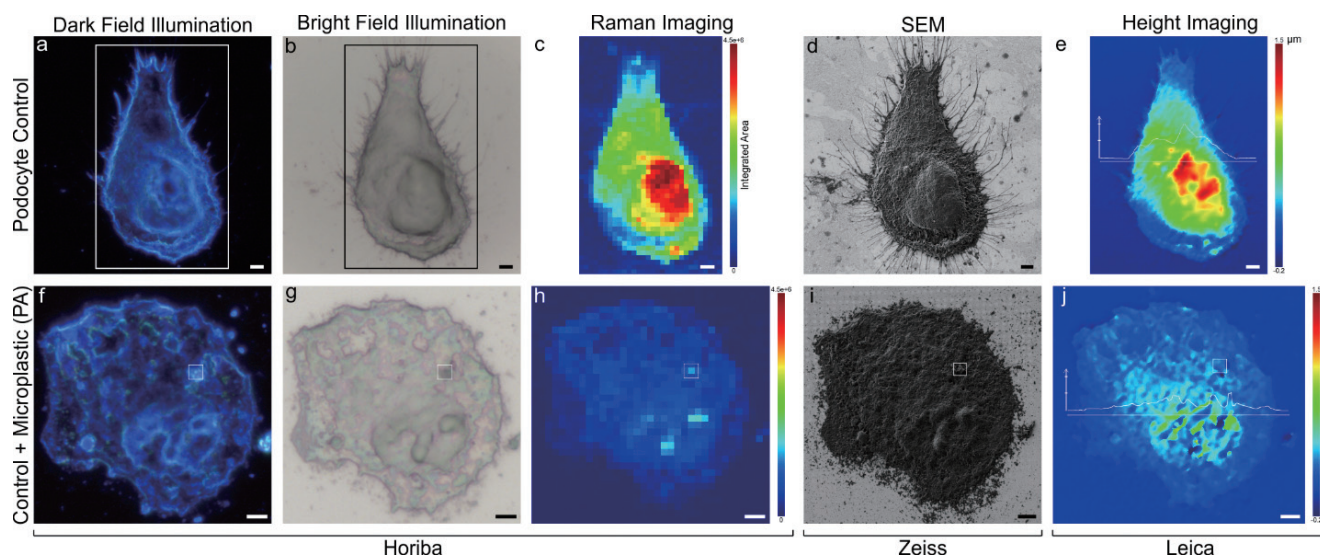

Figure 4   Correlative microscopy and spectroscopy workflow applied to podocytes untreated, control (first row) and particle treated (second row) with 1 mg/ml PA (Table 1 and Figure 3) using the nanoGPS position encoder tag (Figure 1). Two representative cells were easily relocalized and investigated in three independent instruments from different manufactures (Horiba, Zeiss, Leica) with complementary analytical techniques. First, an integrated optical microscope with dark (a, f) and bright (b, g) field illumination and micro-Raman spectrometer are used for a fast visual inspection of cells, followed by Raman imaging (c, h), showing less Raman signal for treated cells (note the same scale) that is an indication of podocytes damage after exposure to PA. Second, SEM imaging (d, i) reveals detailed surface morphology changes at nanoscale induced by the PA treatment and visualizes a PA nanoparticle (~ 30 nm), as confirmed by micro-Raman spectroscopy, delimitated by the square in the second row. Third, an interferometric profilometer is employed to measure the height profile without (e) and with (j) plastic contamination (note the same scale), PA incubated cells being flatter. Two horizontal profiles are also shown (maximum heights of ~ 1.5 μm and ~ 0.8 μm for the control and treated cell, respectively). Scale bars are 3 μm.
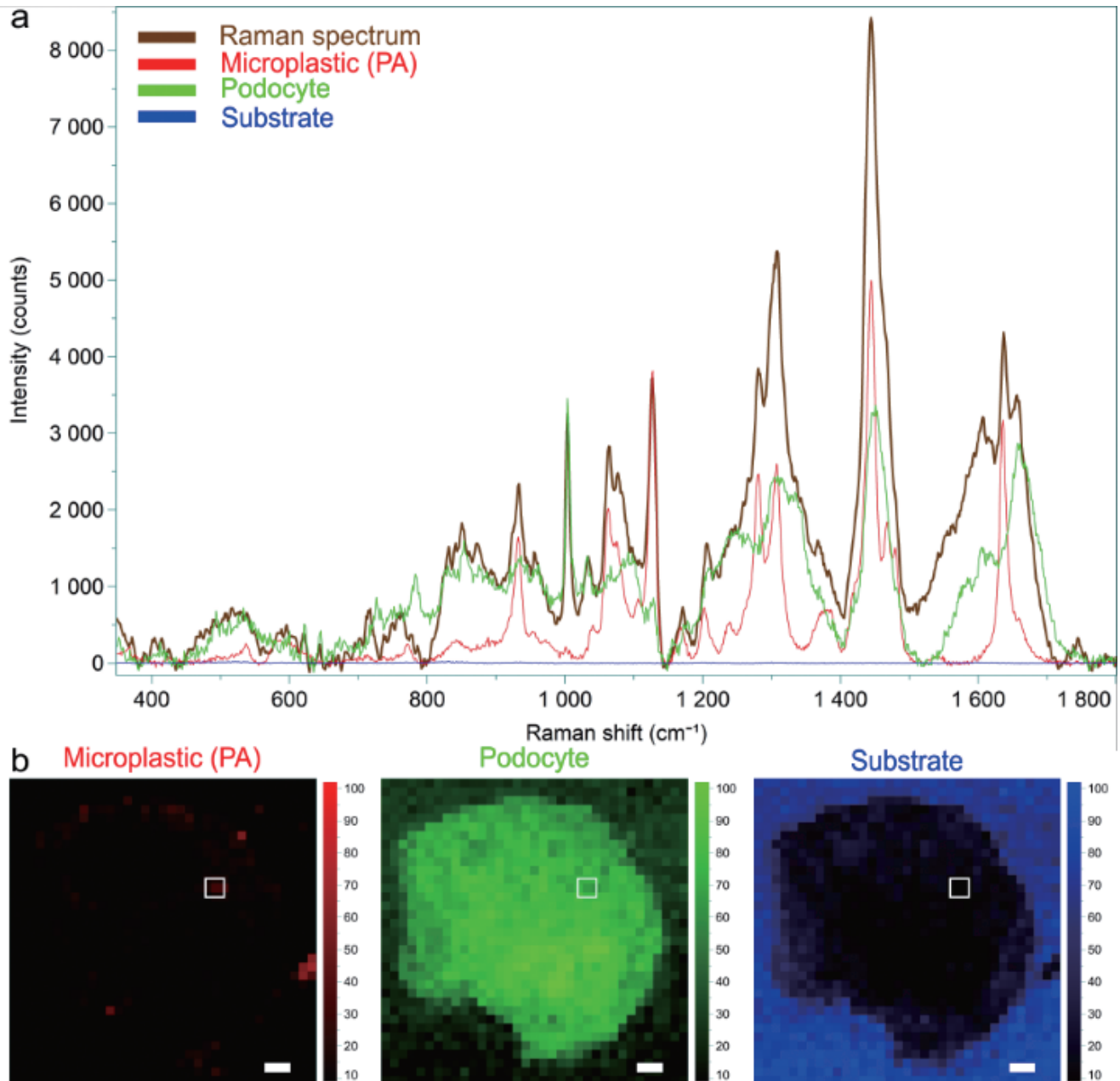
Figure 5 (a) Classical least squares (CLS) fitting is applied to decompose each measured Raman spectrum into its spectral components based on given reference spectra. (b) Separate score maps are generated for each component as illustrated for the podocyte cell treated with PA shown in Figure 4 (second row). The square indicates the position of a PA particle. Thus, despite the superimposed and complex Raman bands of cells and MNP particles, the spatial distribution of MNPs can be clearly localized. Scale bars are 3 µm.

Results and Discussion

nanoGPS relocalization

The nanoGPS relocalization technology for correlative microscopy and spectroscopy investigations is illustrated in Figure 1 for standard micro-sized plastic particles (Table 1), with some particles being by chance < 1 µm. First, a nanoGPS tag is rigidly mounted next to the Al coated PC membrane filter, both on a SEM holder that is moved between instruments, such that the tag and sample keep their positions relative to each other. The smaller the distance between tag and sample, the better the relocalization accuracy that can be further influenced by stage and imaging characteristics. Second, the multiscale and multi-modal patterns on the tag are employed to calibrate the stage of each instrument, different feature sizes being used for distinct instrument magnifications (see SEM image of the entire tag). Three images are taken at random positions on a chosen pattern and fed along with the global, stage coordinates into the NaviGo software. In this example, images were recorded with the 10× objective of the optical microscope on the micro-Raman spectrometer. The software automatically determines the local, sample coordinates and rotation with respect to the tag. This calibration procedure is repeated for all instruments in the workflow and can be recalled anytime by recording one single image on the same pattern, independent of stage and sample rotation.

Guest Forum
特別寄稿

Context Microscopy and Fingerprinting Spectroscopy of Micro- and Nanoplastics and Their Effects on Human Kidney Cells Using nanoGPS and ParticleFinder

In the third step, one or more ROIs are located on the filter and their sample coordinates are saved in one instrument and retrieved in other instruments by converting sample, local into stage, global coordinates. In our case, large-area optical images acquired by stitching under BF and DF illumination are compared to a large field of view SEM image, with the same particle marked on all over-view pictures. Next, MNPs can be directly relocalized and imaged at spatial resolutions of optical and electron microscopies (step four) and their spectral fingerprints determined by micro-Raman spectroscopy (step five) (PP is not shown). While on the BF and DF optical images these particles appear to be single, SEM imaging reveals that PE and PVC are cluster particles. When approaching the filter pore size, particles are barely visible in BF, but clearly noticeable in DF because they shine brighter than the pores, as seen for PVC. Moreover, SEM shows smooth surfaces with spherical and fragment-like shapes for the studied polymer particles. It should be noted that BF, DF, and Raman are usually performed before SEM; however, low-voltage SEM does not damage MNPs, so that Raman after SEM is also possible.[14] All in all, nanoGPS tagging enables sample navigation and observation at different length scales in independent instruments, thus detailed morphological (size, shape, surface, number) and chemical characterization of the same micro- and nanoparticles is achievable.

ParticleFinder

The ParticleFinder software module combined with DF optical microscopy and micro-Raman spectroscopy represents another example of correlative analysis applied here to study contamination by microplastic, pigment, and additive particles in bottled mineral water. 32 samples from 21 different brands of mineral water were investigated to determine the number, size, and type of particles, the results being summarized in Figure 2.[21] DF imaging is used to scan five large-area image montages (1 mm^2) on each sample to warrant significant particle statistics. Such a montage generated by stitching (Figure 2a) is then converted into a grey scale image, on which all particles ≥ 1 μm are automatically detected and individually measured by micro-Raman (Figure 2b).

We identified varying amounts of microplastics in water from all bottle types, partly resulting in large error bars when calculating the mean particle number (Figure 2c); however, some trends are clearly visible. On average, higher number of microplastics were found in water from reusable (PET and glass) compared to single use PET bottles. Interestingly, newish, reusable PET showed less microplastics than older, reusable PET, but similar to single use PET, suggesting that the bottle age can critically affect MP contamination. Regarding the average

size distribution, 90.5% of MPs were ≤ 5 μm in all bottles and ~ 50% were ≤ 1.5 μm in PET bottles (Figure 2d), these MP size classes being addressed for the first time in such samples.[21,24] The predominant polymer type detected in PET bottles was PET considered to originate from the bottle material, while some PET particles displayed olefinic or pigment spectral interferences. In glass bottles, we mainly found PE and PS attributed to abrasion of caps on the glass bottleneck as well as PS, styrene-butadiene-copolymer, and PET most likely from the machinery used for the cleaning process (Figure 2e).

In addition to microplastics, pigmented and additive particles were also detected in the analyzed mineral water samples. Large variations in the number of pigmented particles in water from different bottle and label types were observed (Figure 2f). On average, single use PET contained less pigments similar to blank samples, while reusable PET and glass bottles with printed paper labels showed higher amounts of pigments. Alike MPs, older, reusable PET displayed more pigments than newish, reusable PET and most of the pigmented particles belonged to size classes investigated for the first time, 91.5% were ≤ 5 μm and 45.1% were ≤ 1.5 μm (Figure 2g).[21,24] We found that the pigment types mainly correspond to the colors used for printing on the paper labels (Figure 2h). These pigment particles originate from the paper labels and enter into the bottles during the cleaning process. [25] Additive particles were detected in reusable PET bottles and considered to leach from the bottle material (68.6% were ≤ 5 μm and 11.7% were ≤ 1.5 μm). These results demonstrate that ParticleFinder can be used for automatic detection, classification, and Raman measurement of particles < 1.5 μm from real samples, which is very important due to toxicological reasons, since this size class is considered small enough to penetrate deeply into organs.[21,22]

Effects of MNPs on podocytes

The potential risk of plastic particles on human health is addressed in this study using human podocytes as a highly-specialized kidney cell type. Since kidneys are involved in the filtration process and do not regenerate their cells continuously, they are likely to accumulate MNPs over the lifetime.[26] We performed cell viability tests after incubation of podocytes with four different MNP types (standards PVC, PA, PP, and tyre wear) using a live-dead (green - red) cell fluorescent based kit. Representative results for relevant plastic concentrations after 7 h exposure with respect to control cells are summarized in Figure 3. The cytotoxicity response is found to depend on the polymer type, a higher concentration is needed for PP (5 mg/ml) compared to PVC, PA, and tyre wear (0.5 - 1 mg/ml) to achieve a similar cell mortality rate. Two mechanisms are proposed to explain

the damage induced by the plastic particles on podocytes and finally their death. First, particles can attach on the cell surface and limit the nutrient uptake, the degree of attachment depending on particles' adhesion properties and sizes. Some particles still remained attached after three times washing with PBS following incubation and can be visualized based on their intrinsic fluorescence as shown in Figure 3. Second, smaller size particles can be taken up into the cells by phagocytosis as illustrated in Figure 4 for PA particles.

The correlative microscopy and spectroscopy characterization of identical cells using the nanoGPS relocalization technology is demonstrated in Figure 4, exemplary shown for PA treated cells. Two representative podocytes (control and incubated) are localized in three independent instruments and studied with complementary analytical techniques down to nanoscale resolution. Optical imaging (~ 1 μm spatial resolution) under DF (a, f) and BF (b, g) illumination show the degradation and deformation of cells after particle exposure. The structural damage is further confirmed by micro-Raman mapping (c, h), treated cells display Raman spectra with less intensity (note the same scale for the integrated area maps). High spatial resolution SEM imaging (< 10 nm) is used to assay the integrity of cell features at nanoscale, exposed cells do not regularly show normal biological features like heterogeneous surface, nucleus, and foot processes (d, i). Height profile imaging acquired with an interferometric profilometer quantifies the deformation of incubated cells that flatten with respect to control cells (e, j), with height changes from ~ 0.8 μm to ~ 1.5 μm, respectively (note the same scale). Given the complex peak structure of Raman spectra from cells and plastic particles and the large overlap between peaks, we employed a CLS fitting algorithm that decomposes each measured Raman spectrum into its spectral components and provides score distribution maps for each component as displayed in Figure 5. This enables us to spatially resolved MNPs without underlying podocyte and substrate backgrounds, which are shown separately. Taking advantage of the nanoGPS relocalization capability in a correlative workflow, the same PA particle (outlined by the square in Figure 5b and Figure 4 - second row) was imaged by SEM and found to be a nanoparticle (~ 30 nm) most likely taken up into the cell by phagocytosis (Figure 4i). All in all, these preliminary experiments indicate the negative influence of plastic particles on human podocyte cells; however, more assays are needed to account for other relevant polymers present in the environment and their separate and mixed effects on different human organs, tissues, and cells.

Conclusion

The present study introduces an efficient measurement protocol for the assessment of contamination, accumulation, and hazards related to micro- and nanoplastic particles in bottled mineral water and human kidney cells. This protocol combines context microscopy and fingerprinting spectroscopy with automated relocalization (nanoGPS) and detection (ParticleFinder) of the same MNPs and cells in separate instruments from distinct manufactures (HORIBA, Zeiss, Leica). Results on microparticle contamination (average number, size, type) in mineral water and toxicity effects of MNPs (standards PVC, PA, PP, and tyre wear) on podocytes (in-vitro) are reported. It was found that the bottle material (single use, reusable PET and glass), bottle age (older, newish reusable PET), and label print (paper, plastic) affect the distributions of microplastics, pigments, and additives. In contrast to non-treated controls, podocytes incubated with MNPs tend to lack usual cell characteristics such as heterogeneous surface, nucleus, and foot processes, confirming the potential risk of plastic particles on the viability of cells. These findings were revealed by a biological cell test supported by complementary methods involving optical (bright, dark field) and scanning electron microscopy, micro-Raman spectroscopy (with CLS spectra fitting), and height interferometric profilometry. Further work will deal with different plastic types, concentrations, and exposure times.

* Editorial note: This content is based on HORIBA's investigation at the year of issue unless otherwise stated.

George Sarau and Melina Yarbakht contributed equally to this work.

G uest Forum
特別寄稿

Context Microscopy and Fingerprinting Spectroscopy of Micro- and Nanoplastics and Their Effects on Human Kidney Cells Using nanoGPS and ParticleFinder

References

[1] L. Lebreton, A. Andrady. "Future scenarios of global plastic waste generation and disposal". *Palgrave Commun*. 2019. **5**(1): 6.

[2] R. Geyer, J.R. Jambeck, K.L. Law. "Production, use, and fate of all plastics ever made". *Sci. Adv*. 2017. **3**(7): e1700782.

[3] P.J. Kole, A.J. Löhr, F. Van Belleghem, A. Ragas. "Wear and Tear of Tyres: A Stealthy Source of Microplastics in the Environment". *Int. J. Environ. Res. Public Health*. 2017. **14**(10): 1265.

[4] L.M. Hernandez, N. Yousefi, N. Tufenkji. "Are There Nanoplastics in Your Personal Care Products?" *Environ. Sci. Technol. Lett*. 2017. **4**(7): 280-285.

[5] C.M. Rochman. "Microplastics research—from sink to source". *Science*. 2018. **360**(6384): 28-29.

[6] K. Munno, H. De Frond, B. O'Donnell, C.M. Rochman. "Increasing the Accessibility for Characterizing Microplastics: Introducing New Application-Based and Spectral Libraries of Plastic Particles (SLoPP and SLoPP-E)". *Anal. Chem*. 2020. **92**(3): 2443-2451.

[7] L.M. Hernandez, E.G. Xu, H.C.E. Larsson, R. Tahara, V.B. Maisuria, N. Tufenkji. "Plastic Teabags Release Billions of Microparticles and Nanoparticles into Tea". *Environ. Sci. Technol*. 2019. **53**(21): 12300-12310.

[8] S.L. Wright, F.J. Kelly. "Plastic and Human Health: A Micro Issue?" *Environ. Sci. Technol*. 2017. **51**(12): 6634-6647.

[9] R. Lehner, C. Weder, A. Petri-Fink, B. Rothen-Rutishauser. "Emergence of Nanoplastic in the Environment and Possible Impact on Human Health". *Environ. Sci. Technol*. 2019. **53**(4): 1748-1765.

[10] J.C. Prata, J.P. da Costa, I. Lopes, A.C. Duarte, T. Rocha-Santos. "Environmental exposure to microplastics: An overview on possible human health effects". *Sci. Total Environ*. 2020. **702**: 134455.

[11] W.J. Shim, S.H. Hong, S.E. Eo. "Identification methods in microplastic analysis: a review". *Anal. Methods*. 2017. **9**(9): 1384-1391.

[12] G. Renner, T.C. Schmidt, J. Schram. "Analytical methodologies for monitoring micro(nano)plastics: Which are fit for purpose?" *Curr. Opin. Environ. Sci. Heal*. 2018. **1**: 55-61.

[13] L. Cabernard, L. Roscher, C. Lorenz, G. Gerdts, S. Primpke. "Comparison of Raman and Fourier Transform Infrared Spectroscopy for the Quantification of Microplastics in the Aquatic Environment". *Environ. Sci. Technol*. 2018. **52**(22): 13279-13288.

[14] G. Sarau, L. Kling, B. Ossmann, A.-K. Unger, F. Vogler, S.H. Christiansen. "Correlative Microscopy and Spectroscopy Workflow for Microplastics". *Appl. Spectrosc*. 2020. 000370282091625.

[15] C. Cardell, I. Guerra. "An overview of emerging hyphenated SEM-EDX and Raman spectroscopy systems: Applications in life, environmental and materials sciences". *TrAC Trends Anal. Chem*. 2016. **77**: 156-166.

[16] G. Sarau, M. Heilmann, M. Latzel, C. Tessarek, S. Christiansen. "GaN-Based Nanorods/Graphene Heterostructures for Optoelectronic Applications". *Phys. Status Solidi B*. 2019. **256**(4): 1800454.

[17] G. Sarau, M. Heilmann, M. Latzel, S. Christiansen. "Disentangling the effects of nanoscale structural variations on the light emission wavelength of single nano-emitters: InGaN/GaN multiquantum well nano-LEDs for a case study". *Nanoscale*. 2014. **6**(20): 11953-11962.

[18] G. Sarau, M. Heilmann, M. Bashouti, M. Latzel, C. Tessarek, S. Christiansen. "Efficient Nitrogen Doping of Single-Layer Graphene Accompanied by Negligible Defect Generation for Integration into Hybrid Semiconductor Heterostructures". *ACS Appl. Mater. Interfaces*. 2017. **9**(11): 10003-10011.

[19] G. Sarau, S. Christiansen, M. Holla, W. Seifert. "Correlating internal stresses, electrical activity and defect structure on the micrometer scale in EFG silicon ribbons". *Sol. Energy Mater. Sol. Cells*. 2011. **95**(8): 2264-2271.

[20] S.-A. Strungaru, R. Jijie, M. Nicoara, G. Plavan, C. Faggio. "Micro-(nano) plastics in freshwater ecosystems: Abundance, toxicological impact and quantification methodology". *TrAC Trends Anal. Chem*. 2019. **110**: 116-128.

[21] B.E. Oßmann, G. Sarau, H. Holtmannspötter, M. Pischetsrieder, S.H. Christiansen, W. Dicke. "Small-sized microplastics and pigmented particles in bottled mineral water". *Water Res*. 2018. **141**: 307-316.

[22] B.E. Oßmann, G. Sarau, S.W. Schmitt, H. Holtmannspötter, S.H. Christiansen, W. Dicke. "Development of an optimal filter substrate for the identification of small microplastic particles in food by micro-Raman spectroscopy". *Anal. Bioanal. Chem*. 2017. **409**(16): 4099-4109.

[23] J. Müller-Deile, K. Worthmann, M. Saleem, I. Tossidou, H. Haller, M. Schiffer. "The balance of autocrine VEGF-A and VEGF-C determines podocyte survival". *Am. J. Physiol. Physiol*. 2009. **297**(6): F1656-F1667.

[24] D. Schymanski, C. Goldbeck, H.-U. Humpf, P. Fürst. "Analysis of microplastics in water by micro-Raman spectroscopy: Release of plastic particles from different packaging into mineral water". *Water Res*. 2018. **129**: 154-162.

[25] B.E. Oßmann. "Determination of microparticles, in particular microplastics in beverages". 2020. urn:nbn:de:bvb:29-opus4-132788.

[26] X. Xu, G. Wang, N. Chen, T. Lu, S. Nie, G. Xu, et al. "Long-term exposure to air pollution and increased risk of membranous nephropathy in China". *J. Am. Soc. Nephrol*. 2016. **27**(12): 3739-3746.